

The First Very Long Baseline Interferometry Image of 44 GHz Methanol Maser with the KVN and VERA Array (KaVA)

Naoko Matsumoto¹, Tomoya Hirota^{1,2}, Koichiro Sugiyama³, Kee-Tae Kim⁴,
 Mikyung Kim⁴, Do-Young Byun⁴, Taehyun Jung⁴, James O. Chibueze⁵, Mareki Honma^{1,2},
 Osamu Kameya¹, Jongsoo Kim⁴, A-Ran Lyo⁴, Kazuhito Motogi³, Chungsik Oh⁴,
 Nagisa Shino², Kazuyoshi Sunada¹, Jaehan Bae^{4,6}, Hyunsoo Chung⁴, Moon-Hee Chung⁴,
 Se-Hyung Cho⁴, Myoung-Hee Han⁴, Seog-Tae Han⁴, Jung-Wook Hwang⁴, Do-Heung Je⁴,
 Takaaki Jike¹, Dong-Kyu Jung⁴, Jin-seung Jung⁴, Ji-hyun Kang⁴, Jiman Kang⁴,
 Yong-Woo Kang⁴, Yukitoshi Kan-ya¹, Noriyuki Kawaguchi^{1,2}, Bong Gyu Kim⁴,
 Jaeheon Kim⁴, Hyo Ryoung Kim⁴, Hyun-Goo Kim⁴, Hideyuki Kobayashi¹, Yusuke Kono¹,
 Tomoharu Kurayama^{1,7}, Changhoon Lee⁴, Jeong Ae Lee⁴, Jeewon Lee^{4,8}, Jung-Won Lee⁴,
 Sang Hyun Lee⁴, Sang-Sung Lee⁴, Young Chol Minh⁴, Atsushi Miyazaki⁴, Se-Jin Oh⁴,
 Tomoaki Oyama¹, Sun-youp Park⁴, Duk-Gyoo Roh⁴, Tetsuo Sasao^{1,4,9},
 Satoko Sawada-Satoh¹, Katsunori M. Shibata^{1,2}, Bong Won Sohn⁴, Min-Gyu Song⁴,
 Yoshiaki Tamura¹, Kiyooki Wajima¹⁰, Seog-Oh Wi⁴, Jae-Hwan Yeom⁴, and
 Young Joo Yun⁴

¹Mizusawa VLBI Observatory, National Astronomical Observatory of Japan, 2-21-1 Osawa,
 Mitaka, Tokyo 181-8588, Japan; naoko.matsumoto@nao.ac.jp

²Department of Astronomical Science, The Graduate University of Advanced Studies
 (SOKENDAI),

2-21-1 Osawa, Mitaka, Tokyo 181-8588, Japan

³Graduate school of Science and Engineering, Yamaguchi University, 1677-1 Yoshida,
 Yamaguchi, Yamaguchi 753-8512, Japan

⁴Korea Astronomy and Space Science Institute, Daedeokdae-ro 776, Yuseong-gu, Daejeon
 305-348, Korea

⁵East Asian ALMA Regional Center, National Astronomical Observatory of Japan, 2-21-1
 Osawa, Mitaka, Tokyo 181-8588, Japan

⁶Department of Astronomy, University of Michigan, 500 Church Street, Ann Arbor, MI
48105, USA

⁷Center for Fundamental Education, Teikyo University of Science, 2525 Yatsusawa,
Uenohara, Yamanashi 409-0193, Japan

⁸Department of Astronomy and Space Science, Kyung Hee University, Seocheon-Dong,
Giheung-Gu, Yongin, Gyeonggi-Do 446-701, Korea

⁹Yaeyama Star Club, Ookawa, Ishigaki, Okinawa 904-0022, Japan

¹⁰Shanghai Astronomical Observatory, Chinese Academy of Sciences 80 Nandan Road,
Xuhui District, Shanghai 200030, China

Received 2014 March 14; accepted 2014 May 27

ABSTRACT

We have carried out the first very long baseline interferometry (VLBI) imaging of 44 GHz class I methanol maser ($7_0-6_1A^+$) associated with a millimeter core MM2 in a massive star-forming region IRAS 18151–1208 with KaVA (KVN and VERA Array), which is a newly combined array of KVN (Korean VLBI Network) and VERA (VLBI Exploration of Radio Astrometry). We have succeeded in imaging compact maser features with a synthesized beam size of $2.7 \text{ milliarcseconds} \times 1.5 \text{ milliarcseconds}$ (mas). These features are detected at a limited number of baselines within the length of shorter than $\approx 650 \text{ km}$ corresponding to $100 M\lambda$ in the uv -coverage. The central velocity and the velocity width of the 44 GHz methanol maser are consistent with those of the quiescent gas rather than the outflow traced by the SiO thermal line. The minimum component size among the maser features is $\sim 5 \text{ mas} \times 2 \text{ mas}$, which corresponds to the linear size of $\sim 15 \text{ AU} \times 6 \text{ AU}$ assuming a distance of 3 kpc. The brightness temperatures of these features range from $\sim 3.5 \times 10^8$ to $1.0 \times 10^{10} \text{ K}$, which are higher than estimated lower limit from a previous Very Large Array observation with the highest spatial resolution of $\sim 50 \text{ mas}$. The 44 GHz class I methanol maser in IRAS 18151–1208 is found to be associated with the MM2 core, which is thought to be less evolved than another millimeter core MM1 associated with the 6.7 GHz class II methanol maser.

Subject headings: instrumentation: interferometers — ISM: individual objects (IRAS 18151–1208 MM2) — masers — stars: formation — techniques: high angular resolution

1. Introduction

Methanol masers are known to be associated with star-forming regions. They are classified into two series of transitions called class I and class II (Menten 1991). The class I and II methanol masers are considered to be excited by collisional (e.g., Cragg et al. 1992) and radiative pumping mechanisms (e.g., Sobolev & Deguchi 1994; Cragg et al. 2005), respectively. In general, the class I methanol masers are likely to be associated with interacting regions between outflows and dense ambient gases in both low- and high-mass star-forming regions (e.g., Plambeck & Menten 1990; Kalenskii et al. 2010). In contrast, the class II methanol masers are centrally concentrated around hot molecular cores, ultracompact (UC) HII regions, OH masers and near-IR sources only in high-mass star-forming regions (e.g., Minier et al. 2003; Xu et al. 2008; Cyganowski et al. 2009; Breen et al. 2013), and possibly associated with disk-like structures and outflows around massive young stellar objects (e.g., Bartkiewicz et al. 2009; De Buizer 2003). The class I and II methanol masers are complementary, and proper motion measurements of both maser lines are important to understand three-dimensional velocity structures of massive young stellar objects associated with jet/outflow/circumstellar disk systems. The class I and II methanol masers also hold a possibility of evolutionary tracers, but the relationship between them is still unclear (e.g., Ellingsen et al. 2007; Breen et al. 2010; Fontani et al. 2010).

The $5_1-6_0A^+$ methanol maser at 6.7 GHz is one of the brightest maser species, and classified as the class II. The 6.7 GHz methanol-maser emitting sources have been widely investigated with radio interferometers such as ATCA and Very Large Array (VLA; e.g., Walsh et al. 1998), and very long baseline interferometry (VLBI; e.g., Sugiyama et al. 2008; Bartkiewicz et al. 2009). In contrast, the $7_0-6_1A^+$ methanol maser at 44 GHz is representative of the class I methanol maser. Recently, the 44 GHz methanol masers

have been extensively observed with single-dish radio telescopes and connected-element interferometers (e.g., Kurtz et al. 2004).

However, there is a difficulty in observing the class I methanol masers at high angular resolution. Previous VLBI observations of the class I methanol masers (the $8_0-7_1A^+$ transition at 95.2 GHz: Lonsdale et al. 1998) have failed to detect any fringes for several strong class I methanol maser sources. As the results of the VLA observations (e.g., Slysh et al. 2002; Polushkin et al. 2009) and the negative results of Lonsdale et al. (1998), spot sizes of the class I methanol masers are expected to be between several milliarcseconds (mas) and ~ 50 mas. Because of such extended structures, it has been recognized that the class I methanol masers are easily resolved out and hence, hardly detected with current VLBI instruments with a typical angular resolution of an order of ~ 1 mas. Thus, there was no report for successful imaging of the class I methanol masers with VLBI to date.

Recently, a new VLBI instrument, Korean VLBI Network (KVN) has been constructed, which consists of three 21 m radio telescopes (Lee et al. 2014). Since the maximum baseline length of KVN is ~ 500 km ($\theta_{\text{beam}} \sim 3$ mas at 44 GHz), it is the most suitable for conducting VLBI observations of the 44 GHz class I methanol masers (K. T. Kim et al., in preparation). To conduct high quality VLBI imaging, we extend the array by including four stations of VLBI Exploration of Radio Astrometry (VERA), which is another VLBI network in Japan.

In this Letter, we report on the first result of our VLBI imaging observation of the 44 GHz methanol maser line toward a star-forming region providing the highest angular resolution image. Our target source is one of the brightest 44 GHz methanol maser sources, IRAS 18151–1208 MM2. The distance of this source was estimated to be 3 kpc (Sridharan et al. 2005). This source was detected in the course of a KVN single-dish survey with a total flux density of about 500 Jy (K. T. Kim et al., in preparation), and hence, it is an ideal target to conduct high-resolution VLBI observations with KaVA (KVN and VERA

Array), which is a newly combined array of KVN and VERA, with the longest baseline length of $\sim 2,300$ km (Niinuma et al. 2014).

2. Observation and data reduction

A VLBI observation was carried out on 2012 April 8, from UT 17:10 to 23:53, with KaVA. Our target source was the 44 GHz methanol maser around IRAS 18151–1208 MM2. The phase tracking center position was $\alpha_{J2000.0} = 18^{\text{h}}17^{\text{m}}50^{\text{s}}.1$ and $\delta_{J2000.0} = -12^{\circ}07'48''$. NRAO 530 was observed as a delay and bandpass calibrator. A radio frequency of 44.069410 GHz (Tsunekawa et al. 1995;¹¹ Müller et al. 2004) is adopted in this Letter as the rest frequency of the $\text{CH}_3\text{OH } 7_0-6_1A^+$ transition. Left-hand circular polarization (LHCP) signals were recorded with SONY DIR1000 recorders at a rate of 128 Mbit s^{-1} at all the stations. A correlation process was carried out with the Mitaka FX correlator in NAOJ, Mitaka (Chikada et al. 1991). The resultant auto-correlation and cross-correlation spectra consist of 1024 spectral points with a frequency spacing of 31.25 kHz ($\sim 0.21 \text{ km s}^{-1}$) in two 16 MHz bandwidth channels (1st CH: 44.059–44.075 GHz, 2nd CH 44.075–44.091 GHz in sky frequencies). In addition, both LHCP and RHCP (right-hand circular polarization) signals were recorded with Mark 5B recorders at a rate of 1024 Mbit s^{-1} at all the three KVN stations. They were correlated with the Distributed FX (DiFX; Deller et al. 2007, 2011) software correlator in KASI, Daejeon (Lee et al. 2014). Because we failed to record the data with the DIR1000 recorder at one of the KVN stations, Tamna, we instead employed the Mark 5B/DiFX data for the Tamna baselines and combined with the DIR1000/Mitaka FX data for the other baselines. In this Letter, we only employed two 16 MHz base-band signals of LHCP which are compatible with all the stations.

¹¹<http://www.sci.u-toyama.ac.jp/phys/4ken/atlas/>

Data reduction was performed using the NRAO AIPS package by applying a standard procedure. At first, the two datasets, correlated with DiFX and Mitaka FX, were calibrated separately as follows. The delay and the delay-rate offset were calibrated using NRAO 530. Bandpass responses were also calibrated using NRAO 530. Amplitude calibrations were performed by a template method using the total-power spectra of the 44 GHz methanol maser in IRAS 18151–1208 MM2. Fringe-fitting was conducted for a reference maser component in IRAS 18151–1208 MM2 at a LSR (local standard of rest) velocity, v_{LSR} , of 29.6 km s^{-1} . Then, the datasets were combined after flagging a duplicated baseline in the data correlated with DiFX (the Yonsei-Ulsan baseline). In the self-calibration of the reference maser component, visibility based model-fittings and self-calibrations were iteratively conducted with the DIFMAP software package provided by Caltech to detect faint components from the limited uv -coverage data. The self-calibration solutions were applied to the other velocity channels of the maser data.

Synthesis imaging and deconvolution were performed using DIFMAP with uniform weighting. In this procedure, cut-off signal-to-noise ratios (S/N) of 7–14 were used to avoid possible effects of side-lobes. These cut-off values depend on dynamic ranges of each channel map. The rms noise levels in the deconvolved maps are ~ 50 – 200 mJy for IRAS 18151–1208 MM2. The synthesized beam sizes (FWHM) and the position angle were $2.7 \text{ mas} \times 1.5 \text{ mas}$ and 64° , respectively. For all maser channels, maps were made with $8192 \text{ pixel} \times 8192 \text{ pixel}$ with a pixel size of 0.1 mas . Because of the insufficient velocity resolution and uncertainty in the clean process with our limited uv -coverage, maser structures in the images vary significantly from channel to channel (Figures 1 (a) and (b)). However, we regarded the three maser features identified in multi-channels within the synthesized beam size as real from a comparison between the visibility data and the convolution models. For example, the map of $v_{\text{LSR}} = 29.8 \text{ km s}^{-1}$ in Figure 1 (a) shows a double-peaked structure in a north-south direction while the northern component at $(-2,$

5) position was not detected in neighboring channels. Therefore, this northern component is not considered in the following results and discussions.

Finally, the maser positions, fluxes, and sizes were derived by Gaussian fitting to each maser component in the identified three maser features using the AIPS task JMFIT (Table 1). To avoid influences from complicated structures of weak components, we employed image pixels with the intensity greater than the 90 % of the peak intensity in the fitting. These maser components in the three maser features have S/N greater than 10 as seen in Table 1 and Figures 1 (a) and (b). These peak intensities in the deconvolved maps correspond to 1.4–8.3 times the cut-off S/N in the imaging process.

3. Results

Figure 2 shows spectra of the 44 GHz methanol maser line obtained from our observation. A velocity width of the 44 GHz methanol maser line is around 3 km s^{-1} . The weak red-shifted wing can be seen in the auto-correlation and cross-correlation spectra of the 44 GHz methanol maser (Figure 2). The peak flux density of the 44 GHz methanol maser is $379 \pm 22 \text{ Jy}$ ($v_{\text{peak}} = 30.0 \text{ km s}^{-1}$) in the auto-correlation spectrum. However, the maximum value of the cross-correlation spectrum is $102 \pm 1 \text{ Jy}$ ($v_{\text{peak}} = 29.5 \text{ km s}^{-1}$) in Yonsei-Ulsan baseline at UT 18:46 - 18:47 corresponding to $u \sim 18 \text{ M}\lambda$ and $v \sim 19 \text{ M}\lambda$. Furthermore, except UT 17 h–21 h of Yonsei-Ulsan baseline, peak flux densities of all the baselines are lower than $\sim 20 \text{ Jy}$. Thus, 27 % of the emission can be recovered with our VLBI images and the remaining 73 % is completely resolved out. This means that the 44 GHz methanol maser emission is not a compact point source but is dominated by a spatially extended structure.

Such an extended structure of each feature is also shown in a uv -distance plot (Figure 3). This plot shows a variation of the visibility amplitude with the uv -distance for

the systemic velocity of 29.8 km s^{-1} . There is a decreasing trend of the amplitude within $\sim 27 \text{ M}\lambda$. The data points between $\sim 100\text{--}330 \text{ M}\lambda$ could not be detected in the fringe-fitting process. From Gaussian fitting to this plot along with the flux of auto-correlation spectrum, this trend suggests an extended maser component with a size of $\sim 4 \text{ mas}$. In addition, an increasing trend of the amplitude around $20 \text{ M}\lambda$ suggests an elongated maser structure. The visibility data with the uv -lengths shorter than $20 \text{ M}\lambda$ corresponds to the Yonsei-Ulsan baseline data at UT 17:16 - 18:48. In contrast, visibility amplitudes with the baseline lengths longer than $30 \text{ M}\lambda$ have almost constant values of $\sim 15 \text{ Jy}$, suggesting a spatially compact structure.

Figure 1 (c) shows a spatial and velocity distribution of the 44 GHz methanol maser components. We found three maser features at different LSR velocities, denoted as 1–3. The absolute position of the maser component with $v_{\text{LSR}} = 29.4 \text{ km s}^{-1}$ at $(0, 0)$ position is derived from a fringe-rate mapping using the AIPS task FRMAP to be $\alpha_{J2000.0} = 18^{\text{h}}17^{\text{m}}49^{\text{s}}.95$, and $\delta_{J2000.0} = -12^{\circ}08'06''.5$. Thus, the 44 GHz methanol maser components are separated from the MM2 core position (Beuther et al. 2002a) by $\Delta\alpha \sim 0.4''$ and $\Delta\delta \sim 11.5''$.

As mentioned in Section 1, the 44 GHz methanol maser toward the IRAS 18151–1208 MM2 was detected in the course of KVN single-dish survey observations (K. T. Kim et al. in preparation). The single-dish observation was carried out toward the MM1 position, but the bright maser emission was found to be offset toward the southwest direction. According to the five-point cross-scan, the maser position was identified as the MM2 position with the accuracy of $\sim 5''$. In our VLBI observation, we adopted the coordinates obtained from the single-dish survey. However, the coordinates obtained from the fringe-rate mapping was different from the single-dish result by $\sim 19''$ in a north-south direction, which is larger than the position error. The difference would be caused by a larger uncertainty in the

fringe-rate mapping probably due to our insufficient uv -coverage which made the lines in the fringe-rate map roughly lie north-south directions. Even if the result of the fringe-rate mapping has the error of around $20''$, the maser components detected in our observation are considered to belong to the MM2 region (see Figure 1 of Beuther et al. 2002a).

The radial velocities of these components range from $v_{\text{LSR}} = 29.4$ to 31.1 km s^{-1} . They are spread over an area of $\sim 60 \text{ mas} \times 90 \text{ mas}$ or $\sim 180 \text{ AU} \times 270 \text{ AU}$ at an assumed distance of 3 kpc (Sridharan et al. 2005). We cannot see significant velocity structure indicative of outflow, infall, or rotational motions.

The channel maps are shown in Figures 1 (a) and (b) for the 44 GHz methanol maser features. These maser structures are clearly more extended than the beam size. Their detailed properties are summarized in Table 1. The minimum size among the maser features is $4.98 (\pm 0.32) \text{ mas} \times 2.16 (\pm 0.14) \text{ mas}$ at v_{LSR} of 30.9 km s^{-1} , and the maximum brightness temperature is estimated to be $1.0 \times 10^{10} \text{ K}$ at v_{LSR} of 29.6 km s^{-1} with an uncertainty in the absolute amplitude calibration around a few tens percent in addition to the fitting errors in Table 1.

4. Discussions

We have succeeded in detecting the 44 GHz methanol maser features around the IRAS 18151–1208 MM2 using newly organized KaVA. This is the first VLBI image of the class I methanol maser line at 44 GHz with the highest angular resolution of about 2 mas . Thanks to the high angular resolution, our results suggest that the 44 GHz methanol masers also have compact components with the sizes of a few tens of AU that are detectable by VLBI observations. With further observations of the class I methanol masers, it will be possible to provide three-dimensional velocity maps including radial velocities and

proper motions as well as useful information to reveal the maser pumping mechanisms by comparing positions of multiple methanol maser lines at high spatial resolutions comparable with their spot sizes.

Previously, the highest resolution maps of the 44 GHz methanol masers were reported by Polushkin et al. (2009) for DR21(OH) using VLA with the resolution of 50 mas. They derived the linear sizes of the maser components to be 30–480 AU. Slysh et al. (2002) also reported an upper limit of the maser component size of typically 50 mas, and their linear sizes are less than several hundred AU for five sources with VLA observation with an angular resolution of ~ 100 mas. They showed the lower limit of the brightness temperature of 10^8 K for the strongest masers.

In our VLBI images, the minimum size among the maser features is estimated to be 2–4 mas, and the maximum brightness temperature is estimated to be $\sim 10^{10}$ K. This brightness temperature is much higher by two to four orders of magnitude than those estimated by previous lower resolution observations with VLA (e.g., Kogan & Slysh 1998; Slysh et al. 2002). This is the first case determining the brightness temperature for the class I methanol masers with a sufficiently high spatial resolution, and consistent with the previous suggestions (e.g., Kogan & Slysh 1998; Slysh et al. 2002).

As seen in Figure 2, the central velocity of the 44 GHz methanol maser agrees well with the ambient molecular gas traced by the H^{13}CO^+ thermal line (see Figure 1 of Sakai et al. 2010). Although it is proposed that the 44 GHz methanol maser is excited in the shocked molecular gas, both central velocity and its velocity range are not well correlated with the outflows traced by the SiO thermal line (see Figure 1 of Sakai et al. 2010). It is consistent with previous interpretations for other sources that the class I methanol maser at 95 GHz traces intermediate gas around interaction regions with protostellar outflows and ambient quiescent molecular gas (Plambeck & Menten 1990).

In the IRAS 18151–1208 region, there are four millimeter massive cores labeled MM1 to MM4 (Beuther et al. 2002a) and two of them, MM1 and MM2, are associated with maser emissions (Beuther et al. 2002b). The 6.7 GHz class II methanol maser is detected toward MM1 (e.g., Beuther et al. 2002b), and the 22 GHz H₂O maser is detected toward both MM1 (Valdettaro et al. 2001) and MM2 (Beuther et al. 2002b). These water/methanol maser lines and CO outflows (Marseille et al. 2008) are signposts of young stellar objects.

MM2 is considered as a chemically and dynamically less-evolved massive core than MM1 (e.g., Marseille et al. 2008; Sakai et al. 2010; Chen et al. 2011a; Ragan et al. 2012). MM1 is the birthplace of a massive young stellar object, possibly a pre-UCHII region (e.g., Campbell et al. 2008; Marseille et al. 2008). In fact, around the MM1 position, radio continuum emissions are detected at $\lambda \sim 1.3$ cm (Beuther et al. 2009; Hofner et al. 2011) and 3.6 cm (Carral et al. 1999), which are interpreted as shock-ionized flows/jets rather than UCHII region (Hofner et al. 2011). In contrast, there is no detection of the 6.7 GHz methanol maser or radio continuum at cm-wavelength around the MM2 position.

Based on infrared observations, MM1 is also identified as a high-mass protostellar object with a point source of *MSX* 8 μ m and *Spitzer* 24 μ m emissions (Sakai et al. 2012), while MM2 is an *MSX* dark source and associated with the *Spitzer* 24 μ m emission (Sakai et al. 2012). *Herschel* data also show that MM1 and MM2 are associated with far-infrared point sources in 70–500 μ m images, and MM1 is brighter than MM2 (Ragan et al. 2012). From the *Herschel* data, the masses of MM1 and MM2 cores are estimated to be 106 M_{\odot} and 81 M_{\odot} , respectively (Ragan et al. 2012).

All these characteristics suggest that the evolutionary stage of MM2 could be earlier than MM1. While we cannot rule out a possibility that MM2 does not host any massive young stellar objects judging from a non-detection of the 6.7 GHz class II methanol maser, it is a potential site of massive star formation with a sufficient mass of 81 M_{\odot} . If this is

the case, our result suggests that the 44 GHz class I methanol maser tends to appear in an earlier evolutionary phase than that traced by the 6.7 GHz class II methanol maser in the IRAS 18151–1208 region. It is consistently explained by one of the currently proposed scenarios of the evolutionary phase of massive star-forming regions that the class I methanol masers appear in a younger phase than the class II methanol masers (Ellingsen et al. 2007). However, other observational studies claimed another trend in which the class I methanol masers may be associated with more than one evolutionary stage (i.e., hot core and UCHII) during formation of massive young stellar objects (Voronkov et al. 2010; Chen et al. 2011b; Cyganowski et al. 2012). One possible reason for such a discrepancy would be insufficient spatial resolutions employed in some of the survey observations with single-dish telescopes, which could be affected by the complicated structure of massive star-forming regions as found in our target source IRAS 18151–1208. Thus, further high-angular resolution observations of a much larger sample of methanol maser sources are required to discuss the evolutionary stage of massive young stellar objects with maser species. VLBI observations of the 44 GHz methanol masers will be powerful tools to provide their accurate positions and proper motions, which are crucial to identifying the powering source of masers.

We are grateful to all staff members and students at the KVN and VERA who helped to operate the array and to correlate the data. The KVN is a facility operated by the Korea Astronomy and Space Science Institute. VERA is a facility operated by National Astronomical Observatory of Japan in collaboration with Japanese universities. We also appreciate Dr. T. Sakai and Dr. S. Kameno for useful comments.

Facilities: VERA, KVN

REFERENCES

- Bartkiewicz, A., Szymczak, M., van Langevelde, H. J., Richards, A. M. S., & Pihlström, Y. M. 2009, *A&A*, 502, 155
- Beuther, H., Schilke, P., Menten, K. M., et al. 2002a, *ApJ*, 566, 945
- Beuther, H., Walsh, A., Schilke, P., et al. 2002b, *A&A*, 390, 289
- Beuther, H., Walsh, A. J., & Longmore, S. N. 2009, *ApJS*, 184, 366
- Breen, S. L., Ellingsen, S. P., Caswell, J. L., & Lewis, B. E. 2010, *MNRAS*, 401, 2219
- Breen, S. L., Ellingsen, S. P., Contreras, Y., et al. 2013, *MNRAS*, 435, 524
- Campbell, M. F., Sridharan, T. K., Beuther, H., et al. 2008, *ApJ*, 673, 954
- Carral, P., Kurtz, S., Rodríguez, L. F., et al. 1999, *RMxAA*, 35, 97
- Chen, H.-R., Liu, S.-Y., Su, Y.-N., & Wang, M.-Y. 2011a, *ApJ*, 743, 196
- Chen, X., Ellingsen, S. P., Shen, Z.-Q., Titmarsh, A., & Gan, C.-G. 2011b, *ApJS*, 196, 9
- Chikada, Y., Kawaguchi, N., Inoue, M., et al. 1991, *Frontiers of VLBI*, ed. H. Hirabayashi, M. Inoue, & H. Kobayashi (Tokyo: Universal Academy Press), 79
- Cragg, D. M., Johns, K. P., Godfrey, P. D., & Brown, R. D. 1992, *MNRAS*, 259, 203
- Cragg, D. M., Sobolev, A. M., & Godfrey, P. D. 2005, *MNRAS*, 360, 533
- Cyganowski, C. J., Brogan, C. L., Hunter, T. R., & Churchwell, E. 2009, *ApJ*, 702, 1615
- Cyganowski, C. J., Brogan, C. L., Hunter, T. R., et al. 2012, *ApJL*, 760, L20
- De Buizer, J. M. 2003, *MNRAS*, 341, 277

- Deller, A. T., Brisken, W. F., Phillips, C. J., et al. 2011, *PASP*, 123, 275
- Deller, A. T., Tingay, S. J., Bailes, M., & West, C. 2007, *PASP*, 119, 318
- Ellingsen, S. P., Voronkov, M. A., Cragg, D. M., et al. 2007, in *IAU Symp. 242, Astrophysical Masers and Their Environments*, ed. J. M. Chapman & W. A. Baan (Cambridge: Cambridge Univ. Press), 213
- Fontani, F., Cesaroni, R., & Furuya, R. S. 2010, *A&A*, 517, A56
- Hofner, P., Kurtz, S., Ellingsen, S. P., et al. 2011, *ApJL*, 739, L17
- Kalenskii, S. V., Johansson, L. E. B., Bergman, P., et al. 2010, *MNRAS*, 405, 613
- Kogan, L., & Slysh, V. 1998, *ApJ*, 497, 800
- Kurtz, S., Hofner, P., & Álvarez, C. V. 2004, *ApJS*, 155, 149
- Lee, S.-S., Petrov, L., Byun, D.-Y., et al. 2014, *AJ*, 147, 77
- Lonsdale, C. J., Doleman, S. S., Liechti, S., et al. 1998, *BAAS*, 30, 1355
- Marseille, M., Bontemps, S., Herpin, F., van der Tak, F. F. S., & Purcell, C. R. 2008, *A&A*, 488, 579
- Menten, K. 1991, in *ASP Conf. Ser. 16, Atoms, Ions and Molecules: New Results in Spectral Line Astrophysics*, ed. A. D. Haschick & P. T. P. Ho (San Francisco, CA: ASP), 119
- Minier, V., Ellingsen, S. P., Norris, R. P., & Booth, R. S. 2003, *A&A*, 403, 1095
- Müller, H. S. P., Menten, K. M., Mäder, H. 2004, *A&A*, 428, 1019
- Niinuma, K., Lee, S.-S., Kino, M., et al., *PASJ*, submitted
- Plambeck, R. L., & Menten, K. M. 1990, *ApJ*, 364, 555

- Polushkin, S. V., Val'tts, I. E., & Slysh, V. I. 2009, *ARep*, 53, 113
- Ragan, S., Henning, T., Krause, O., et al. 2012, *A&A*, 547, A49
- Sakai, T., Sakai, N., Furuya, K., et al. 2012, *ApJ*, 747, 140
- Sakai, T., Sakai, N., Hirota, T., & Yamamoto, S. 2010, *ApJ*, 714, 1658
- Slysh, V. I., Val'tts, I. E., & Kalenskii, S. V. 2002, in *IAU Symp. 206, Cosmic Masers: From Protostars to Black Holes*, ed. V. Migenes & M. J. Reid (San Francisco, CA: ASP), 199
- Sobolev, A. M., & Deguchi, S. 1994, *A&A*, 291, 569
- Sridharan, T. K., Beuther, H., Saito, M., Wyrowski, F., & Schilke, P. 2005, *ApJL*, 634, L57
- Sugiyama, K., Fujisawa, K., Doi, A., et al. 2008, *PASJ*, 60, 23
- Tsunekawa, S., Ukai, T., Toyama, A., & Takagi, K. 1995, Toyama University. Microwave Frequencies of the CH₃OH Molecule in the Frequency Range from 7 to 200 GHz, report for the Grant-in-aid for Scientific Research on Priority Areas (Interstellar Matter, 19911994) of the Ministry of Education, Science, and Culture, Japan (Toyama: Toyama Univ.)
- Valdettaro, R., Palla, F., Brand, J., et al. 2001, *A&A*, 368, 845
- Voronkov, M. A., Caswell, J. L., Ellingsen, S. P., & Sobolev, A. M. 2010, *MNRAS*, 405, 2471
- Walsh, A. J., Burton, M. G., Hyland, A. R., & Robinson, G. 1998, *MNRAS*, 301, 640
- Xu, Y., Li, J. J., Hachisuka, K., et al. 2008, *A&A*, 485, 729

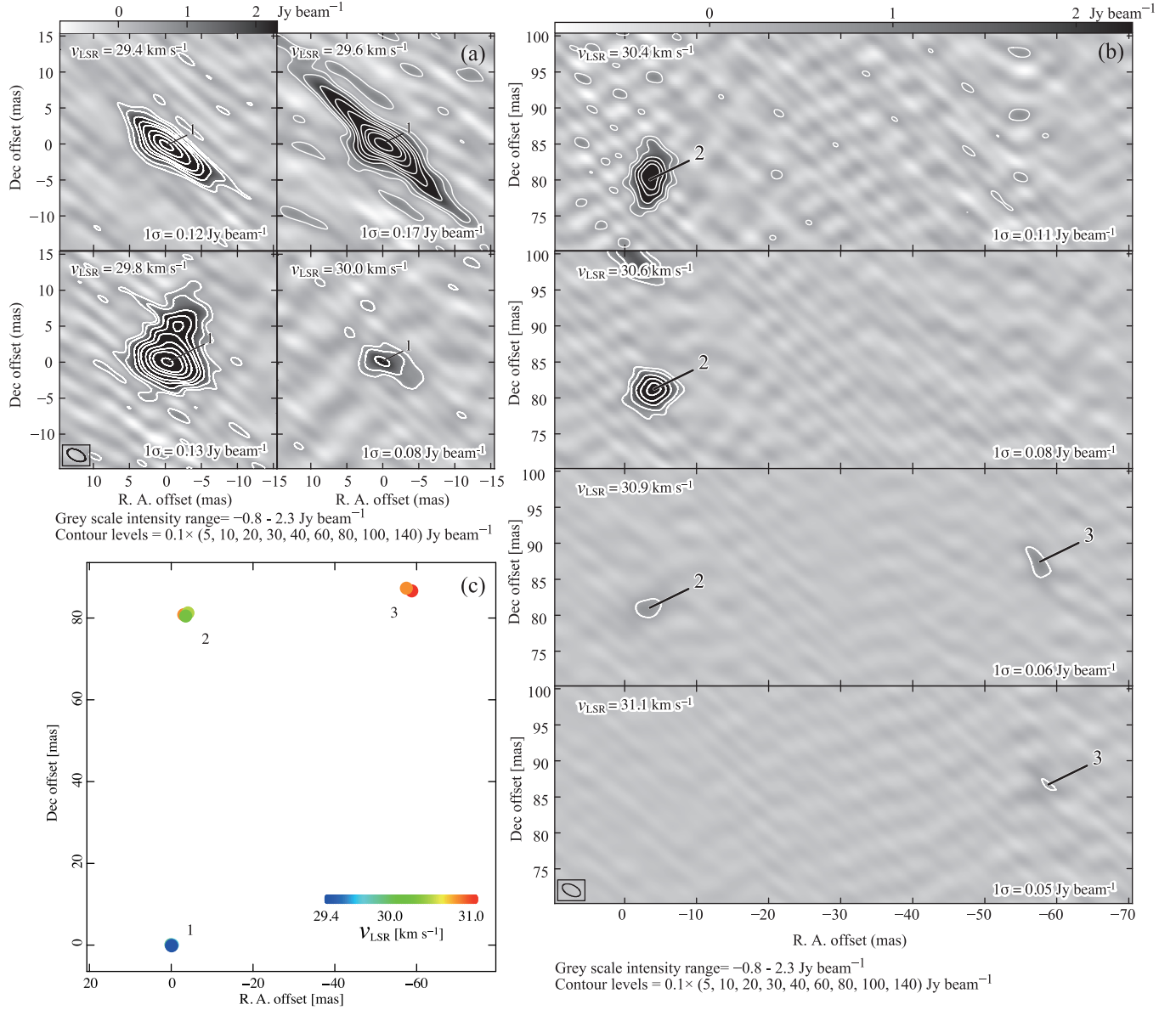


Fig. 1.— (a) Multi-channel intensity maps of the feature 1, (b) same as (a) but for the features 2 and 3, and (c) a velocity map of the CH_3OH ($7_0-6_1A^+$) maser emission toward the IRAS 18151–1208 MM2. The origin of these maps are $\alpha_{J2000.0} = 18^{\text{h}}17^{\text{m}}50^{\text{s}}.0$ and $\delta_{J2000.0} = -12^{\circ}08'07''$ with the errors of $\sim 20''$.

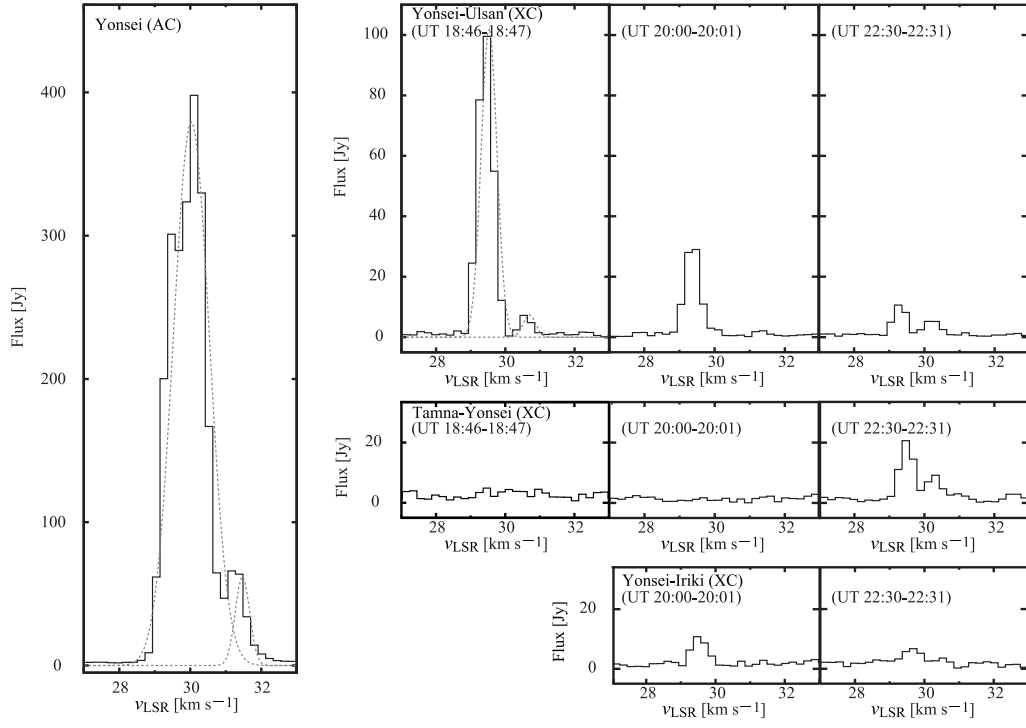


Fig. 2.— Spectra of 44 GHz methanol maser lines of auto-/cross-correlation (AC/XC). Dashed lines are Gaussian components obtained by the method of least squares.

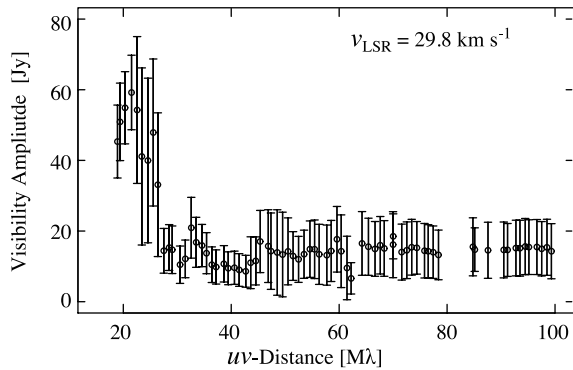


Fig. 3.— The uv -distance plots for visibility amplitude of a CH_3OH ($7_0-6_1A^+$) maser component toward the IRAS 18151–1208 MM2 at a v_{LSR} of 29.8 km s^{-1} .

Table 1: List of Identified maser components

Feature	v_{LSR}	$\Delta\alpha$	$\Delta\delta$	Peak Intensity	Component size	P. A.	T_{peak}
ID	[km s^{-1}]	[mas]	[mas]	[Jy beam^{-1}]	[mas]	[$^{\circ}$]	[$\text{K} \times 10^8$]
1	29.4	-0.10 (3)	-0.19 (2)	10.74 (12)	7.01×2.51 (8, 3)	55.1 (4)	67.5 (8)
1	29.6	-0.07 (2)	-0.07 (2)	16.33 (17)	6.03×2.52 (6, 3)	59.9 (4)	103 (1)
1	29.8	-0.27 (2)	0.03 (1)	14.90 (12)	5.61×3.13 (5, 3)	65.8 (5)	93.7 (8)
1	30.0	0.09 (8)	0.12 (5)	2.30 (9)	5.10×2.29 (19, 9)	63.4 (17)	14.4 (5)
2	30.4	-3.53 (3)	80.52 (5)	5.43 (10)	6.39×3.73 (12, 7)	162.3 (13)	34.2 (6)
2	30.6	-4.06 (3)	81.25 (3)	4.49 (8)	4.96×3.91 (8, 7)	120.8 (29)	28.2 (5)
2	30.9	-3.06 (14)	80.82 (10)	0.74 (6)	4.30×3.15 (32, 24)	82.8 (96)	4.68 (35)
3	30.9	-57.50 (9)	87.32 (12)	0.87 (6)	4.98×2.16 (32, 14)	32.5 (28)	5.46 (35)
3	31.1	-58.82 (21)	86.62 (18)	0.55 (1)	6.70×2.14 (62, 20)	50.3 (27)	3.45 (3)

Note. — The numbers in parentheses represent the standard deviation in the Gaussian fit in units of the last significant digits.